

## Protecting Agricultural Land in Developing Countries: A Case Study from Lahore, Pakistan

Ather Ashraf, Muhammad Imran and Anam Shahbaz

Center for Geographical Information Systems, University of the Punjab, Lahore, Pakistan

Publication Date: 22 August 2015

Article Link: <http://technical.cloud-journals.com/index.php/IJARSG/article/view/Tech-428>



Copyright © 2015 Ather Ashraf, Muhammad Imran and Anam Shahbaz. This is an open access article distributed under the **Creative Commons Attribution License**, which permits unrestricted use, distribution, and reproduction in any medium, provided the original work is properly cited.

**Abstract** Agricultural land needs to be protected for food production. Our objective is to provide a decision support for protecting the agricultural land in Lahore, Pakistan. To do so, first we classified the Land Use and Land Cover (LULC) from Landsat images for the years 2009 and 2012. Second, we performed Markov chain analysis to simulate the LULC change over time. The resultant probability of LULC inter conversion was then combined with the Cellular Automata (CA). Third, the spatio-temporal patterns of LULC change from CA-Markov were integrated with the land fitness map obtained through the analysis of soil chemical properties. We observed a gradual increase in built-up land and a decrease in agricultural land from years 2009 to 2012, with an increase of 18.8% to 60.3% in the built-up land, and a decrease of 43.5% to 35.9% in the agricultural land. The Markov-CA analysis further predicted a significant ( $p = 0.69$ ) LULC change from year 2012 to year 2015, with an increase of 2% in built-up land, and a decrease of 1.3% in agricultural land. The resultant map shows zones to be predicted on priority bases, which can be useful in making comprehensive land policies to protect agricultural land and to secure food in developing countries.

**Keywords** *Land Use and Land Cover (LULC) Change; Enhanced Vegetation Index (EVI); Cellular-Automata Markov-Chain (CA-Markov) Analysis; Soil Suitability Analysis; Protected Agricultural Zones*

### 1. Introduction

In developing countries, agriculture mainly contributes to the economic development. For instance, in Pakistan, about 70% people in rural areas depend on agriculture for their livelihood. Being the major economic activity, it contributes 21.4% to the country's Gross Domestic Product (GDP), and employs 45% of the country's labor force (MOF, 2014). Agricultural farming mainly ensures food and financial viability of individuals, and thus reduces poverty and food in-security (Imran et al., 2014). Urban expansion, on the other hand, is an immense stress on the agricultural land to be turned into the built-up urban land (De Jong et al., 2014). People generally migrate towards the urban areas for better health, education, transportation and employment opportunities, etc. Protecting agricultural land however should be the highest priority to sustain agriculture and to secure enough food (SEMCOG, 2003). Land-suitability analyses are often performed to find agricultural zones to be protected on the priority bases (Xiaoli et al., 2009). This however should be combined with the Land Use and Land

Cover (LULC) change analysis to predict the agricultural zones that are at a risk of being converted into the built-up zones. Examining jointly the predicted LULC patterns and the mapped extents of suitable agricultural land can help finding the land to be protected on priority bases (Bobade et al., 2010).

Spatio-temporal analysis of LULC change has widely been performed using multi-temporal remote sensing (RS), due to its high spatial and temporal coverage (Jat et al., 2008). It usually investigates quantitatively the spatial and temporal changes in land-cover. RS-derived vegetation indices (VIs) are often used to assess the quality and quantity of existing vegetation, and, thus, delineating the agricultural land (Lunetta et al., 2006). Sensitivity of VIs however varies with nature of canopy (Tucker et al., 1991), topographic effects, e.g., slope, aspect and with background soil reflectance (Dorigo et al., 2007). Moreover, they require suitable methods to properly quantify the temporal effects, and thus, the extent of LULC change. RS alone therefore is not sufficient to map an agricultural LULC change. For this, VIs are often combined with various modeling approaches like Automated Artificial Neural Network (Paola et al., 1997; Yuan et al., 2009), Markov Analysis (Iacono et al., 2012), Bayesian statistics (Seto et al., 2002), etc. Through defining discrete-event processes, the stochastic modeling approaches can model a complex and dynamic spatial phenomenon like LULC change. Combining RS and stochastic modeling with Geographical Information System (GIS) proved useful in analyzing the spatio-temporal dynamics of land use change (Agarwal et al., 2002; Falahatkar et al., 2011).

Stochastic processes of LULC change are modeled spatio-temporally to assess the rate and extent of converting agricultural land into built-up land. Markov-chain, for instance, is often used for describing a land use system that follows a chain of linked events or states (Cabral et al., 2009). It calculates the transition probabilities associated with these states in the form of a transition matrix. Markov chain however cannot explicitly model the spatial interactions between elements of the system (Silvertown et al., 1992). Moreover, it cannot account the causes or constraints of LULC change. To overcome this, Cellular Automata (CA) can be used to spatialize the quantitative predictions of LULC change from stochastic models, and thus, to obtain the prediction maps in space and time (Balzter et al., 1998; Soares-Filho et al., 2002; Falahatkar et al., 2011). In this way, the spatial process of interaction between the elements of land use system can be ruled by the transition probabilities from the Markov-chain and other causes of land use change. This study adopts this approach to model LULC change from converting agricultural land into built-up urban land.

To spatially delineate the protected agricultural land for a sustainable urban growth, the quantitative measures of predicted LULC patterns are often linked with land suitability maps. To this end, land quality is generally measured through certain suitability constraints based on a specific crop requirement and land characteristics like salinity, water logging, ravines, degraded hills, and rock quarries (Malczewski et al., 2004). Other factors include modernization of small agricultural land (Sallaku et al., 2009), water availability, e.g., irrigation (Reshmidevi et al., 2009), access to water reservoirs (Steiner et al., 2000), and physio-chemical soil properties (Bobade et al., 2010). This study used soil properties of electric conductivity (EC), Power of Hydrogen (pH), Organic Matter (OM), Phosphorous (P), Potassium (K), and Texture (T), being a widely used method for mapping land suitability in our study area.

Our main objective here is to predict the agricultural lands that are in danger zone of converting into built-up urban land and to quantify the land suitability so that the valuable agricultural land can be protected on priority bases. To do so, we combined RS and GIS with CA-Markov. The study was conducted using the Landsat images and LULC data from Pakistan for the years 2009 to 2013. Pakistan is facing rapid urban growth at the cost of primary agricultural land. First, RS-derived temporal images are classified using visualization techniques. Second, using Markov analysis, the LULC change probabilities are identified from these classified images. Third, CA is applied to spatialize the predicted LULC changes. Fourth, the basic soil chemical properties are examined to

define land suitability constraints. Finally, the predicted maps of land use change are linked to land-suitability maps to obtain the protection zone maps. The protection zone maps developed in this research are highly useful for land managers and urban planners for land use planning while protecting the quality agricultural land in developing countries.

## 2. Study Area

This study was conducted in Lahore, one of the Pakistan's largest cities (Figure 1). It is the world's 30th largest populated city with total population of approximately 10 million and total area of 177204 (ha) (GOP, 2014). Because of an immense increase in the industrial and economic growth, Lahore is facing a high migration rate from suburbs and other cities, causing significance conversion of agricultural land into built-up urban land. Construction of new settlements, roads, factories and other non-agricultural facilities in the city has already utilized agricultural land.

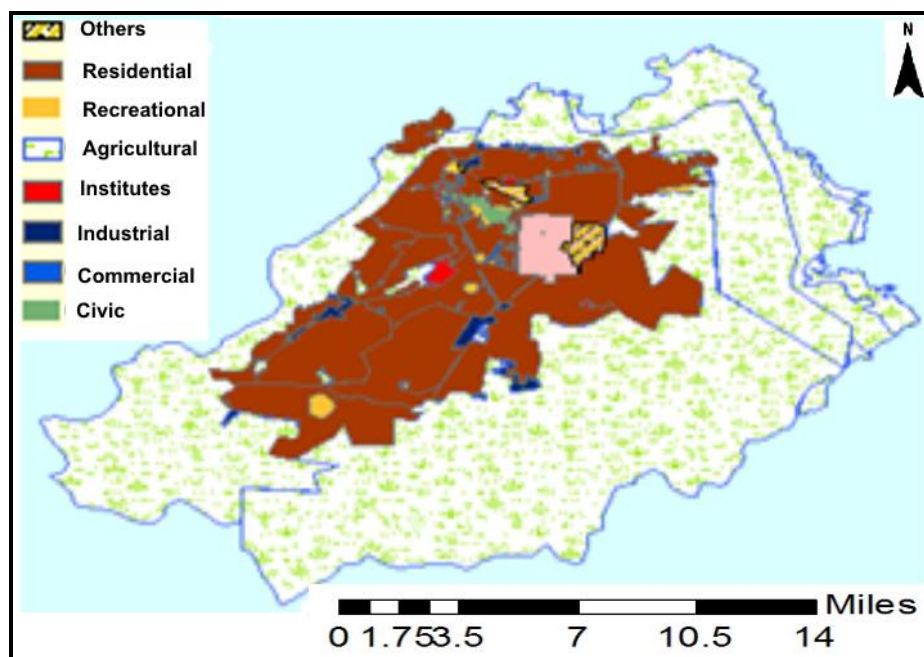


*Figure 1: Agricultural and Built-Up Regions in Lahore in the Year 2011*

In 1972, total areas of cultivated agricultural and uncultivated urban land were equal to 166862 (ha), 10342 (ha), respectively. Due to an intense urban expansion the cultivated land reduced to 163413 (ha) in the year 1980, to 114298 (ha) in the year 1990, to 81040 (ha) in the year 2000 and to 52232 (ha) in the year 2010 (Baloch et al., 2011). Thus, from year 1972 to 2010, the cultivated agricultural land reduced from 94.2% to 29.5% of total land in the study area. (Figure 1) shows the agricultural and built-up regions in the study area in the year 2011.

## 3. Materials and Methods

### 3.1. Data

Two images from Landsat TM and ETM sensors (30 m; 1 year) were obtained for the years 2009 and 2012 (NASA, 2003) to delineate agricultural land in the study area. For the same period, Google-Earth imagery (0.6 m) were obtained for the land use classification purpose. It helps identifying various land use (e.g. industry and water bodies) in the Landsat images. Data on soil chemical properties were obtained from Soil Fertility Research Institute (SFRI), including electric conductivity (EC), pH, organic

matter (OM), Potassium (k), Phosphorus (P), and soil texture (T) (SRI, 2013). The observed quantities were interpolated on a 30 m grid for the study area using ordinary kriging (OK).

### 3.2. Methods

#### 3.2.1. Determining Agricultural Land

Enhanced Vegetation Index (EVI) enhances sensitivity for vegetation in agricultural land through reducing the soil and atmospheric effects (Huete et al., 2006). EVI was used to delineate agricultural land in the study area. It was calculated from the Landsat images for the years 2009 and 2012, as,

$$EVI = G * \frac{(NIR - R)}{(NIR + C1 * R - C2 * B + L)} \quad (1)$$

where NIR is the spectral reflectance in the near-infrared where canopy reflectance is dominant, and R is the reflectance in the red portion of the electromagnetic spectrum where chlorophyll absorbs strongly, and were corrected atmospherically by setting the coefficients with values used in recent land-cover change studies (Wardlow et al., 2007), as,

- Gain factor G: 2.5, i.e., a factor to limit EVI to a fixed range.
- Coefficients of vaporize conflict C1 and C2: 6 and 7, respectively, i.e., the coefficients to adjust vaporizer pressures in the red and blue bands, respectively.
- The reflectance in the blue portion of the electromagnetic spectrum B to minimize the soil and atmospheric effects.
- Soil tuning L: 1, i.e., a function for canopy background adjustment (Huete et al., 2006).

#### 3.2.2. Classifying the RS-Derived EVI Images

To delineate various land-use areas in the study area, regions of low and high EVI were classified through the visual interpretation and using the Jenks natural breaks. High vegetation areas were assigned agriculture land class, whereas the built-up class was assigned to the areas where EVI is zero or very low. Moreover, the industrial areas were identified from the digitized map of Google-Earth. The digitization was performed through converting Google vector maps to the raster maps of the resolution similar to that of the classified images (i.e. 30 m). For the next analysis, we assumed that the agricultural land around the study area are consistently decreasing and converting into the built-up or industrial land.

#### 3.2.3. Conducting Markov-Chain Analysis

To model LULC change over time, Markov-chain analysis was performed on the classified images of the study area for years 2009 and 2012:

$$n_{t+1} = P n_t \quad (2)$$

where  $n_t$  and  $n_{t+1}$  are vector matrices of land use classes at time  $t$  and  $t+1$  with dimension  $m \times 1$ , representing the land use distribution over  $m$  different states (i.e. land use classes), and  $P$  is a  $m \times m$  transition probability matrix between each pair of  $m$  land use classes  $i$  and  $j$ , such that sum of probabilities in each row  $i$  of the transition matrix equals to 1, i.e.,

$$\sum_{j=1}^m P_{ij} = 1; i=1, 2, \dots, m \quad (3)$$

The transition probability matrix was calculated using cross tabulation technique, which resulted the transition area matrix. Further dividing sum of rows with the each matrix element ( $i, j$ ) value resulted the transition probability matrix. The resulting matrix was then multiplied by the vector matrix of current land use class to model the land use classes for the year 2015.

**3.2.4. Obtaining Conditional Probability Images and Applying Cellular Automata (CA)**

The conditional probability images represent the distribution of a land use class given a particular outcome of the other class. The conditional probability images were calculated for each land use class. These  $m$  conditional probability images were overlaid and used as input to CA. CA takes the probability images as input and identifies the predicted patterns. Conditional probability images were calculated by integrating the results of Markov-chain analysis and seed image, where the seed image represents the current land use class.

$$P_z(A|X) = \frac{A}{\sum_{i=1}^m P_{ij}} \tag{4}$$

Where  $A$  is the pixel value of seed image and  $X$  is the sum of column elements of a particular land use class in the transition probability matrix. Markov-chain results into a matrix that needs to be spatialized. To do so, CA was used to model the land use change and to predict future patterns in the spatial domain. For this it was used in loop, such that each iteration of the loop provides the probability  $P_z$  for a pixel or cell ( $x, y$ ) to be zoned for agricultural protection. CA works on a grid cells and finds the change in the state of each cell (Li & Yeh, 2001), as

$$S_{t+1} = f(S_t, N) \tag{5}$$

Where  $f$  is some neighborhood function over the probability images to define change patterns from time  $t$  to  $t+1$ . The neighborhood function works like a kernel that calculates the neighboring values, and assigns the results to the central cell under the kernel window. The dominant neighborhood pattern predicts state at time  $t+1$ . Here we used the contingency filter, as

$$\begin{pmatrix} 00100 \\ 01110 \\ 11111 \\ 01110 \\ 00100 \end{pmatrix}$$

$S_t$  is the current pixel state in the seed image and  $N$  is the neighborhood pattern of all pixels under the contingency filter.

**3.2.5. Defining Land Fitness Surfaces and Obtaining Protection Zone Maps**

Land were evaluated by analyzing the chemical properties of soils, including soil power of Hydrogen (pH), electric conductivity (EC), organic matter (OM), Potassium (K), Nitrogen (N), and Saturation Percentage (SP). Sample data were used to develop the surface of each properties of soil using OK. These surfaces were then classified using importance ranks assigned to each class, as shown in Table 1 (SRI, 2013). Next, the classes were assigned value between 0 and 1, as,

$$C_v = \frac{I_r}{n} \quad (6)$$

Where  $C_v$  is class value,  $I_r$  is the importance rank and  $n$  is the number of classes of a particular property. The class value acted as weight of the soil property. The final land fitness surface, is developed by overlay all the surface and averaging values at each pixel, as

$$LF_v = \frac{1}{n} \sum W_i \quad (7)$$

Where  $LF_v$  is the Land fitness value,  $W_i$  is the weight of particular property, and  $n$  is the number of soil properties.

A suitability map was prepared by overlaying and multiplying the predicted map, i.e., output of CA, and land fitness surface. Before overlaying, the predicted map was converted into a Boolean raster with cell value 1 and 0 for agricultural and non-agricultural land, respectively. Such that the multiplication of these two raster data sets provide a raster having value between 0 to 1 within an agriculture zone.

The final protection zone map was prepared by applying threshold to land fitness surface. Since there was no particular threshold value for defining suitability, we used different threshold values, i.e., 0.5, 0.6 and 0.7 and generated three protection zone maps against each threshold value.

**Table 1: Classes of Soil Chemical Properties**

| Soil Chemical Properties   | Soil Class           | Range (pH) | Imp Rank <sup>a</sup> | Class Value |
|----------------------------|----------------------|------------|-----------------------|-------------|
| Power of Hydrogen (pH)     | Non-Calcareous       | 7.1-7.5    | 1                     | 0           |
|                            | Calcareous Soil      | 7.5-8      | 2                     | 0.33        |
|                            | Alkaline Soil        | 8-8.5      | 3                     | 0.66        |
|                            | Alkali Soil          | > 8.5      | 4                     | 1           |
| Electric conductivity (EC) | Non-Saline           | 0-4        | 4                     | 1           |
|                            | Slightly Saline Soil | 4-8        | 3                     | 0.66        |
|                            | Moderately Saline    | 8-16       | 2                     | 0.33        |
|                            | Highly Saline        | >16        | 1                     | 0           |
| Organic matter (OM)        | Poor                 | 0-0.86     | 1                     | 0           |
|                            | Satisfactory         | 0.86-1.29  | 2                     | 0.5         |
|                            | Adequate             | >1.29      | 3                     | 1           |
| Phosphorus (P)             | Very low             | 0-3.5      | 1                     | 0           |
|                            | Low                  | 3.5-7      | 2                     | 0.25        |
|                            | Medium               | 7-14       | 3                     | 0.5         |
|                            | Satisfactory         | 14-24      | 4                     | 0.75        |
|                            | Adequate             | >21        | 5                     | 1           |
| Potassium (K)              | Very low             | 0- 40      | 1                     | 0           |
|                            | Low                  | 40- 80     | 2                     | 0.33        |
|                            | Satisfactory         | 80- 180    | 3                     | 0.66        |
|                            | Adequate             | >180       | 4                     | 1           |
| Texture (T)                | Sandy                | 0-19       | 1                     | 0           |
|                            | Sandy Loam           | 20-30      | 1                     | 0           |
|                            | Loam                 | 31-45      | 4                     | 1           |
|                            | Clay Loam            | 45-60      | 3                     | 0.5         |

<sup>a</sup>Importance rank

## 4. Results

### 4.1. Determining Agricultural Land

Figure 2 shows the EVI images calculated for the years 2009 and 2012. Comparing the two images, a decrease in vegetation from 2009 to 2012 can be seen on the Eastern part of the study area, showing an immense conversion of agricultural land into the built-up land.

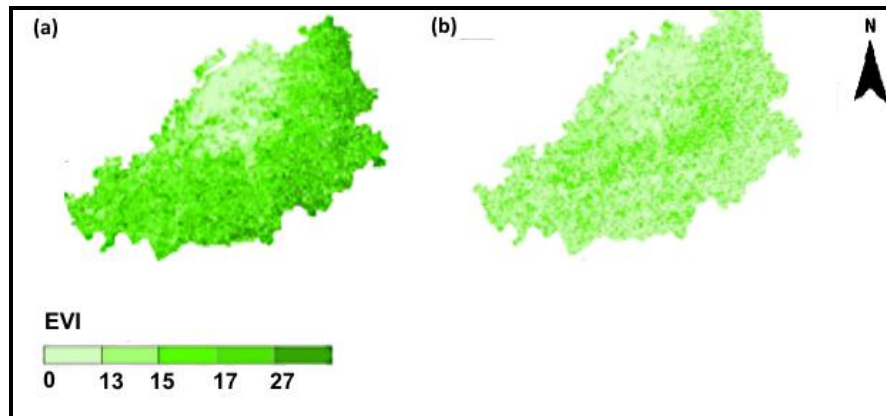


**Figure 2:** Enhanced Vegetation Index (EVI) Values for Year 2009 (a), and Year 2012 (b)

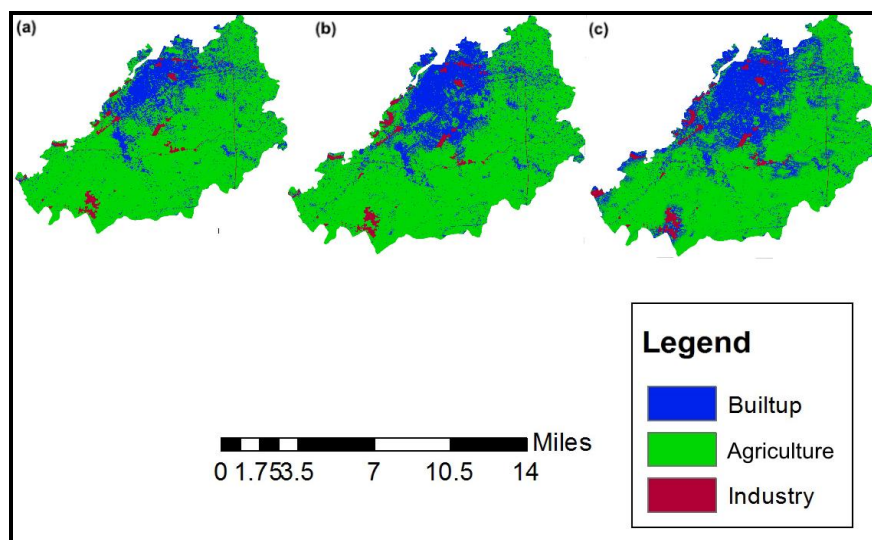


**Figure 3:** Classified Maps of Land-Use Land-Cover (LULC): Initial (a) 2009 (b), 2012 (c)

### 4.2. Classifying the RS-derived EVI Images

Figure 3 shows the classified EVI images. For year 2006, Figure 3 (a) initially differentiates three major land classes as built-up, agriculture, and industry. Figures 3 (b) and 3 (c) show a gradual increase in built-up land and a decrease in agricultural land from years 2009 to 2012, with an increase of 18.8% to 60.3% in the built-up land, and a decrease of 43.5% to 35.9% in the agricultural land. This clearly indicates an increasing trend of urbanization which may cause a major decrease in the primary agricultural land in the study area in future.

#### 4.3. Conducting Markov-Chain Analysis

The probability matrix of transition from year 2009 to 2012 (Appendix A) obtained from the Markov analysis shows a significant probability ( $p = 0.54$ ) of converting agricultural land into the built-up land, and a probability ( $p = 0.44$ ) of no conversion. Whereas the probability matrix of transition from year 2012 to 2015 (Appendix B) shows a significant probability ( $p = 0.69$ ) of converting agricultural land into the built-up land, and a probability ( $p = 0.2967$ ) of no conversion. This shows a high probability of decreasing agriculture land and increasing the built-up land in the study area in the year 2015 compared to the year 2012.

#### 4.4. Obtaining Conditional Probability Images and Applying Cellular Automata (CA)

To find the predicted land use patterns, the conditional probability images of land use (see Figure 4) are used as input to CA. The highest values show low condition probability of a land use class given a particular outcome of another class.

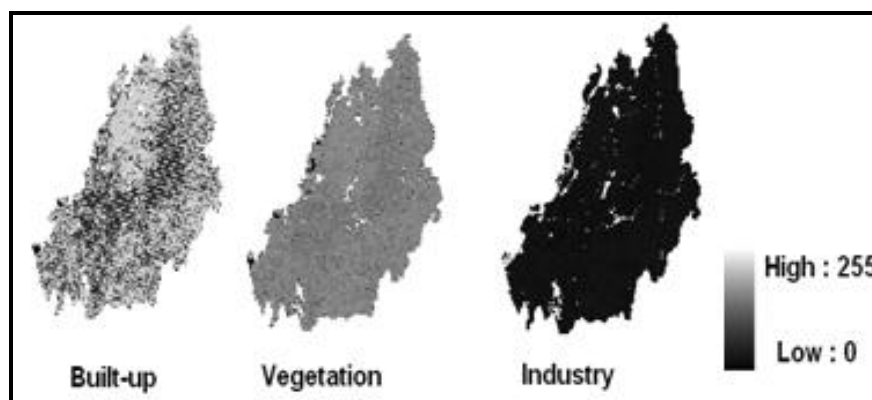


**Figure 4:** Conditional Probability Images of Land-Use Classes

Figure 5 shows the land use distribution predicted for year 2015 with 62.3% built-up, 34.6% agriculture and 1.6% industry of the total land in the study area. The overall LULC change from year 2012 to year 2015 examined an increase of 2% in built-up land use, and a decrease of 1.3% in agricultural land use, and 0.36% in industry land use. The predicted LULC classification shows minimization of industry and agricultural lands while a rapid growth of urban sprawl and increase in built-up land. There is a decrease in industrial land, which may be due to a shift of industry outside the study area.

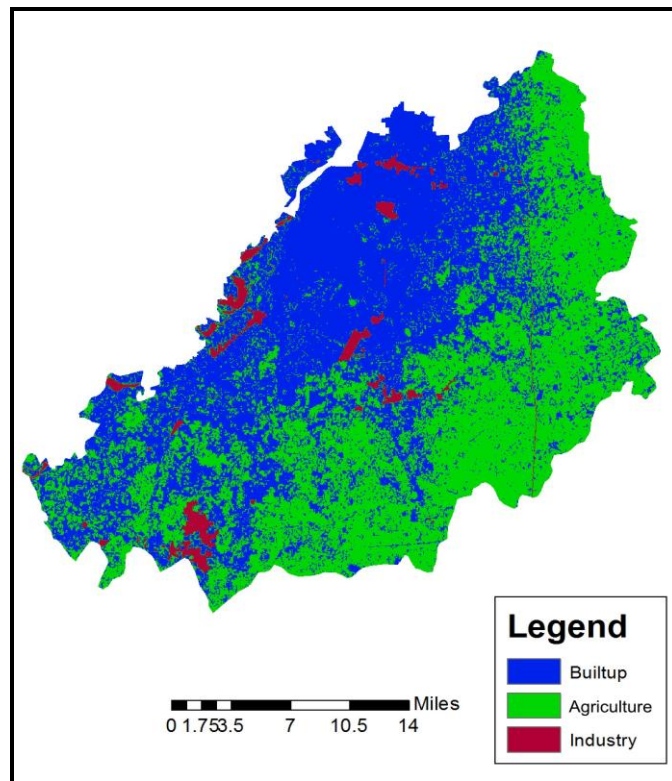


Figure 5: Land-Use Distribution Predicted for Year 2015

#### 4.5. Defining Land Fitness Surfaces and Obtaining Protection Zone Maps

The interpolated and classified soil surfaces are shown in Figure 6 (a). Based on these classified surfaces, the land fitness surfaces are shown in Figure 6 (b). For instance, based on Ph and EC values, land in the study area is classified as non-saline calcareous and alkaline.

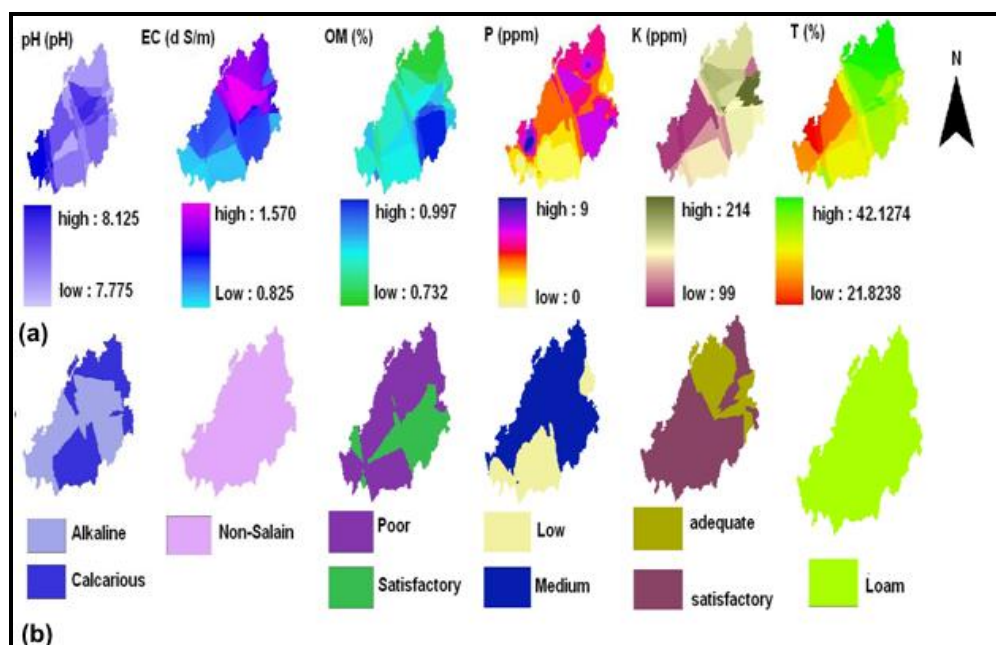
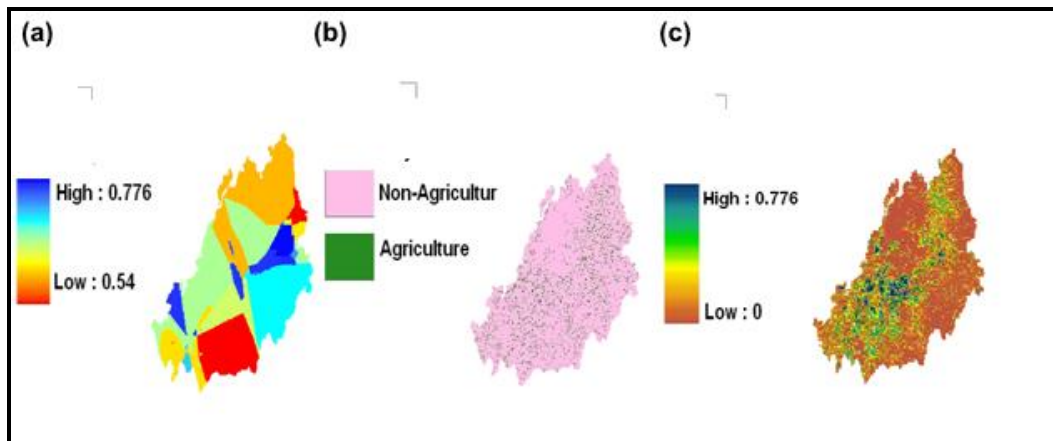


Figure 6: The Interpolated and Classified Soil Surfaces (a); Land Fitness Surfaces (b)



**Figure 7:** Final Land Fitness Surface Obtained from Overlaying All Land Fitness Surfaces in Figure 6(b) and Averaging Values at Each Pixel (a); A Boolean Raster Map Obtained from the Output of Cellular Automata (CA) (b); A Suitability Map Obtained by Overlaying and Multiplying These Two Surfaces (c)

Similarly, the land are classified as poor and satisfactory based on OM values, as low and medium based on P values, and as satisfactory and adequate based on K values. The soil texture however classified the whole study area as loamy. Figure 7(a) shows the final land fitness surface obtained from overlaying all the land fitness surfaces and averaging values at each pixel.

Figure 7(c) shows the suitability map obtained from overlaying and multiplying the final land fitness surface and the Boolean raster map obtained from the output of cellular automata (CA). Figures 8(a-c) show the protection zone maps by applying threshold to land fitness surface, with threshold values equal to 0.5, 0.6, and 0.7, respectively.

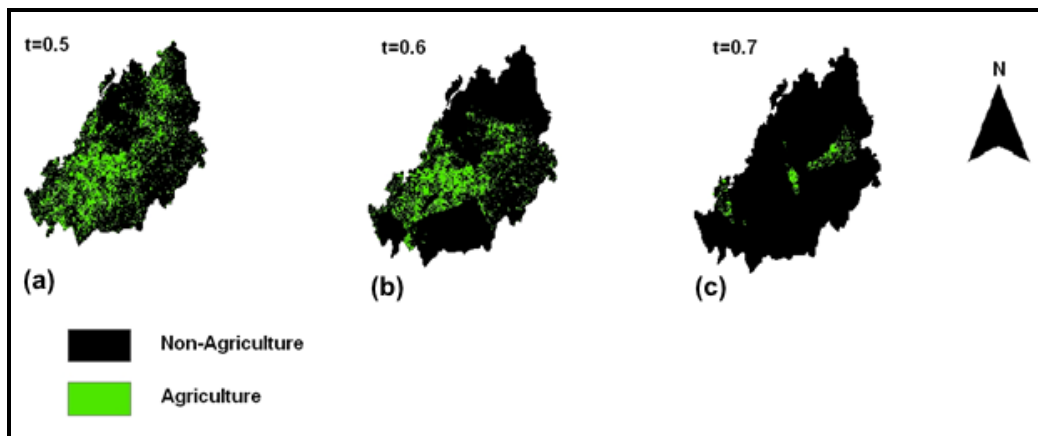


**Figure 8:** Protection Zone Maps by Applying Threshold Value 0.5 (a); 0.6 (b); and 0.7 (c)

## 5. Discussion

Patterns of LULC are modeled and predicted in space and time to protect converting agricultural land to built-up. To do so, spatial data modeling is integrated with stochastic modeling. Predicted patterns are then linked with the soil chemical properties to find the protected zones, i.e., zones that are at a higher risk of conversion and need to be protected.

The visual inspection of EVI time-series gives useful information on the agriculture status in the study area in different years. It shows a dominant increase in the built-up land at the cost of primary agricultural land. For instance, dense vegetation observed in the Eastern part is enormously reduced

from years 2009 to 2012. Western and North-East parts are also dominated by the built-up land use. EVI images are further classified to obtain exact areas of three land use classes, i.e., built-up, agriculture and industry. Agriculture land that was comprised of 43% of the study area in the year 2009 is decreased to 35.9% in the year 2012. This shows a high rate of urbanization in the study area.

In this study, LULC changes are simulated using Markov chain analysis. It assumes the LULC as a stochastic process and different LULC classes become states of the Markov transition probability matrix. The resulting matrix shows a probability equals to 0.5 of changing agriculture land into built-up and a probability equals to 0.4 of sustaining in the agriculture state during the period from 2009 to 2012. During the period from 2012 to 2015, however, these probabilities are equal to 0.6 and 0.2, respectively. This shows that probability of sustaining agriculture land is continuously reducing with time. The Markov analysis is integrated with CA to visualize the quantitative result in space. This results a LULC map of year 2015.

Soils in the study area are nutritiously rich for the agricultural use. Soils are classified through the weight analysis of soil chemical properties that results into a land fitness map of areas having rich soils for agriculture. To define protected zones, the fitness map is further integrated with the predicted agricultural patterns to obtain the final protection zone map. In addition to the soil chemical properties, other suitability factors can be investigated in future, for instance, socio-economic factors (e.g., population pressure, income levels and agricultural production), biophysical factors (e.g., climate and topographical factors) and proximity factors (e.g., distance to roads, water bodies, and settlements).

## 6. Conclusion

This research investigated CA-Markov (Cellular Automata-Markov) for the spatial and temporal analysis to quantify urban growth in Lahore, Pakistan, and, consequently, predicting the conversion of agricultural land into built-up land. It applied Markov-chain to RS-derived classified map of Land-Cover and Land-Use (LULC) to model land use change from year 2009 to year 2012. This output was then integrated with the current land use classes to obtain conditional probability images, which were provided as input to CA to predict land use patterns in the year 2015.

The study showed that the agricultural land are continuously decreased from the year 2009 to 2012. The projected land use in 2015 showed that overall the built-up land will increase 62.3% and the agricultural land will decrease 34.6% of the total land of study area. The results indicate that rapid urbanization is a consistent threat of converting the agricultural land into built-up land. It was therefore required to identify the agriculture zones that need to be protected on priority bases. To do so, the CA-Markov was overlaid with land fitness surface based on soil properties. Results showed that such priority zones mostly exist in the Western, South Western, and North Eastern regions of the study area. The method developed in this research enables to simulate the spatial growth with different development view points and future expansion scenarios can be produced that are useful for policy makers. Urban planners, for instance, can make master plans, providing comprehensive development guidance for future developments in the urban and built-up lands, while preserving agricultural land.

## References

Agarwal, C., Green, G.M., Grove, J.M, Evans, T.P. and Schweik, C.M. 2002: *A Review and Assessment of Land-Use Change Models: Dynamics of Space, Time, and Human Choice*. Gen. Tech. Rep. NE-297. Newton Square, PA: U.S. Department of Agriculture, Forest Service, Northeastern Research Station. 61.

Baloch, A.A. *Urbanization of Arable Land in Lahore City in Pakistan: A Case-Study*. Canadian Social Science. 2011. 7 (4) 58–66.

- Balzter, H., Braun, P.W. and Kohler, W. *Cellular Automata Models for Vegetation Dynamics*. Ecological Modelling. 1998. 107; 113–125.
- Bobade, S.V., Bhaskar, B.P., Gaikwad, M.S., Raja, P., Gaikwad, S.S., Anantwar, S.G., Patil, S.V., Singh, S.R. and Maji, A.K. *A GIS-Based Land Use Suitability Assessment in Seoni District, Madhya Pradesh, India*. Tropical Ecology. 2010. 51 (1) 41–54.
- Cabral, P. and Zamyatin, A. *Markov Processes in Modeling Land Use and Land Cover Changes in SINTRA-CASCAIS, PORTUGAL*. Dyna. 2009. 76 (158) 191–198.
- De Jong, G.F., Aphichat, C. and Quynh-Giang, T. *For Better, for Worse: Life Satisfaction Consequences of Migration*. International Migration Review. 2002. 36 (3) 838–864.
- Dorigo, W.A., Zurita-Milla, R., de Wit, A.J.W., Brazile, J., Singh, R. and Schaepman, M.E. *A Review on Reflective Remote Sensing and Data Assimilation Techniques for Enhanced Agroecosystem Modeling*. Int J Appl Earth Obs. 2007. 9; 165–193.
- GOP, 2014: Punjab Portal, Technical Report, Government of Punjab, Pakistan. [online] <http://www.punjab.gov.pk/>, Accessed on 17 Sep. 2014.
- Falahatkar, S., Soffianian, A.R., Khajeddin, S.J., Ziaee, H.R. and Ahmadi, N.M. *Integration of Remote Sensing Data and GIS for Prediction of Land Cover Map*. Geomatics and Geosciences. 2011. 1 (4) 847–864.
- Huete, A.R. and Tucker, C.J. *Investigation of Soil Influences in Avhrr Red and Near-Infrared Vegetation Index Imagery*. International Journal of Remote Sensing. 1991. 12 (6) 1223–1242.
- Huete, A.R., Didan, K., Shimabukuro, Y.E., Ratana, P., Saleska, C.R., Hutyra, L.R., et al. *Amazon Rainforests Green-Up with Sunlight in Dry Season*. Geophysical Research Letters. 2006. 33; L06405.
- Lacono, M., Levinson, D., El-Geneidy, A. and Wasfi, R., 2012: *Markov Chain Model of Land Use Change in the Twin Cities* Technical report, University of Minnesota: Nexus Research Group. [online] <http://ideas.repec.org/p/nex/wpaper/markovlu.html>, Accessed on 17 Sep. 2014.
- Imran, M., Stein, A. and Zurita-Milla, R. *Investigating Rural Poverty and Marginality in Burkina Faso Using Remote Sensing-Based Products*. International Journal of Applied Earth Observation and Geoinformation. 2014. 26.
- Jat, M.K., Garg, P.K. and Khare, D. *Monitoring and Modelling of Urban Sprawl Using Remote Sensing and GIS Techniques*. International Journal of Applied Earth Observation and Geoinformation. 2008. 10 (1) 26–43.
- Li, X. and Yeh, A.G.O. *Zoning Land for Agricultural Protection by the Integration of Remote Sensing, GIS, and Cellular Automata*. Photogrammetric Engineering and Remote Sensing. 2001. 67 (4) 471–478.
- Lunetta, R.S., Knight, J.F., Ediriwickrema, J., Lyon, J.G. and Worthy, L.D. *Land-Cover Change Detection Using Multi-Temporal {MODIS} {NDVI} Data*. Remote Sensing of Environment. 2006. 105 (2) 142–154.
- Malczewski, J. *GIS-Based Land-Use Suitability Analysis: A Critical Overview*. Progress in Planning. 2004. 62; 3–65.

MOF, 2014: *Pakistan Economic Survey 2012–13, Agriculture Division* Technical report, Ministry of Finance, Islamabad, Pakistan. [online]. [http://www.finance.gov.pk/survey\\_1213.html](http://www.finance.gov.pk/survey_1213.html), Accessed on 17 Sep. 2014.

NASA, 2003: *NASA Landsat Program, 2003 Landsat TM and ETM, SLC-Off*, USGS, Sioux Falls.

Paola, J.D. and Schowengerdt, R.A. *The Effect of Neural-Network Structure on a Multispectral Land-Use/Land-Cover Classification*. Photogrammetric Engineering & Remote Sensing. 1997. 63 (5) 535–544.

Reshmidevi, T.V., Eldho, T.I. and Jana, R. *A GIS-Integrated Fuzzy Rule-Based Inference System for Land Suitability Evaluation in Agricultural Watersheds*. Agricultural systems. 2009. 101 (1) 101–109.

Sallaku, F., Huqi, B., Tota, O., Mema, M., Fortuzp, S. and Jojic, E. *Dynamics of Land-Use and Land-Cover Change in Albania: Environmental Consequences and Policy Response*. Research Journal of Agricultural Science. 2009. 41 (2) 190–198.

SEMCOG, the Southeast Michigan Council of Governments, 2003: *Land Use Tools and Techniques: A Handbook for Local Communities* Technical report, Michigan Department of Transportation, USA. [online]. <http://www.hrwc.org/>, Accessed on 17 Sep. 2014.

Seto, K.C., Woodcock, C.E., Song, C., Huang, X., Lu, J., and Kaufmann, R.K. *Monitoring land-use change in the Pearl River Delta using Landsat TM*. International Journal of Remote Sensing. 2002. 23 (10) 1985–2004.

Silvertown, J., Holtier, S., Johnson, J. and Dale, P. *Cellular Automaton Models of Interspecific Competition for Space - The Effect of Pattern on Process*. Journal of Ecology. 1992. 80; 527–534.

Soares-Filho, B.S., Cerqueira, G.C. and Pennachin, C.L. *Dinamica- A Stochastic Cellular Automata Model Designed to Simulate the Landscape Dynamics in an Amazonian Colonization Frontier*. Ecological Modelling. 2002. 154 (3) 217–235.

SFRI, 2013: *Soil Fertility Research Institute (SFRI) Technical Report*, Government of Punjab, Pakistan. [online] [<http://www.sfripunjab.gov.pk/>], Accessed on 17 Sep. 2014.

Steiner, F., McSherry, L. and Cohen, J. *Land Suitability Analysis for the Upper Gila River Watershed*. Landscape and Urban Planning. 2000. 50 (4) 199–214.

Wardlow, B.D., Egbert, S.L. and Kastens, J.H. *Analysis of Time-Series MODIS 250 M Vegetation Index Data for Crop Classification in the U.S. Central Great Plains*. Remote Sensing of Environment. 2007. 108; 290–310.

Xiaoli, L., Chen, Y. and Daoliang, L.A. *Spatial Decision Support System for Land-use Structure Optimization*. W. Trans. on Comp. 2009. 8 (3) 439–448.

Yuan, H., Van Der Wiele, C.F. and Khorram, S. *An Automated Artificial Neural Network System for Land Use/Land Cover Classification from Landsat TM Imagery*. Remote Sensing. 2009. 1 (3) 243–265.

**Appendix****Appendix A**

Markov Transition Probability Matrix (2009-2012)

|                     | <i>Built – up</i> | <i>Agricultural</i> | <i>Industry</i> |
|---------------------|-------------------|---------------------|-----------------|
| <i>Built – up</i>   | 0.81              | 0.180               | 0.001           |
| <i>Agricultural</i> | 0.54              | 0.440               | 0               |
| <i>Industry</i>     | 0.02              | 0.003               | 0.980           |

**Appendix B**

Markov Transition Probability Matrix (2012-2015)

|                     | <i>Built – up</i> | <i>Agricultural</i> | <i>Industry</i> |
|---------------------|-------------------|---------------------|-----------------|
| <i>Built – up</i>   | 0.76              | 0.23                | 0.002           |
| <i>Agricultural</i> | 0.69              | 0.30                | 0.002           |
| <i>Industry</i>     | 0.04              | 0.01                | 0.960           |